the plant journal

The Plant Journal (2022) 110, 166–178 doi: 10.1111/tpj.15663

Osa-miR535 targets *SQUAMOSA promoter binding protein-like 4* to regulate blast disease resistance in rice

Ling-Li Zhang[1,2,¶], Yan-Yan Huang[1,¶], Ya-Ping Zheng[1,¶], Xin-Xian Liu[1], Shi-Xin Zhou[1], Xue-Mei Yang[1], Shou-Lan Liu[1], Yan Li[1], Jin-Lu Li[1,†], Sheng-Li Zhao[1,‡], He Wang[1], Yun-Peng Ji[1], Ji-Wei Zhang[1], Mei Pu[1], Zhi-Xue Zhao[1], Jing Fan[1] and Wen-Ming Wang1 *

[1]*State Key Laboratory of Crop Gene Exploration and Utilization in Southwest China, Sichuan Agricultural University at Wenjiang, 211 Huimin Road, Chengdu, Sichuan, 611130, China, and*

[2]*College of Environmental Science & Engineering, China West Normal University, 1 Shida Road, Nanchong, Sichuan, 637002, China*

Received 12 July 2021; accepted 2 January 2022; published online 8 January 2022.

*For correspondence (e-mail j316wenmingwang@sicau.edu.cn).

[¶]These authors contributed equally to this work.

[†]Present address: College of Plant Protection, Yunnan Agricultural University, 95 Jinhei Road, Kunming, Yunnan, 650201, China

[‡]Present address: Institute of South Subtropical Crops, Chinese Academy of Tropical Agricultural Sciences, Zhanjiang, Guangdong, 524013, China

SUMMARY

Many rice microRNAs have been identified as fine-tuning factors in the regulation of agronomic traits and immunity. Among them, Osa-miR535 targets *SQUAMOSA promoter binding protein-like 14* (*OsSPL14*) to positively regulate tillers but negatively regulate yield and immunity. Here, we uncovered that Osa-miR535 targets another *SPL* gene, *OsSPL4*, to suppress rice immunity against *Magnaporthe oryzae*. Overexpression of Osa-miR535 significantly decreased the accumulation of the fusion protein $SPL4_{TBS}$-YFP that contains the target site of Osa-miR535 in *OsSPL4*. Consistently, Osa-miR535 mediated the cleavage of *OsSPL4* mRNA between the 10th and 11th base pair of the predicted binding site at the 3′ untranslated region. Transgenic rice lines overexpressing *OsSPL4* (OXSPL4) displayed enhanced blast disease resistance accompanied by enhanced immune responses, including increased expression of defense-relative genes and up-accumulated H_2O_2. By contrast, the knockout mutant *osspl4* exhibited susceptibility. Moreover, OsSPL4 binds to the promoter of *GH3.2*, an indole-3-acetic acid-amido synthetase, and promotes its expression. Together, these data indicate that *Os*-miR535 targets *OsSPL4* and *OsSPL4-GH3.2*, which may parallel the *OsSPL14-WRKY45* module in rice blast disease resistance.

Keywords: *Oryza sativa*, Osa-miR535, transcription factor, OsSPL4, *Magnaporthe oryzae*, GH3.2.

INTRODUCTION

The microRNAs (miRNAs), a class of small non-coding RNAs with 20–24 nucleotides, are encoded by miRNA genes (*MIRs*) and mature subsequently by a series of processes including splicing and methylation (Diederichs et al., 2009; Li, Jeyakumar, et al., 2019b). The mature miRNAs are loaded to ARGONAUTEs to form miRNA-induced gene silencing complexes, which target the sequence of mRNAs guided by miRNA in a sequence-complementary manner, and suppress gene expression via transcript cleavage or translational inhibition (Li, Jeyakumar, et al., 2019b; Yu et al., 2017). Subsequent to the miRNA being first identified in nematodes in 1993 (Lee et al., 1993; Wightman et al., 1993), it was widely found in most forms of life (Pfeffer et al., 2004). miRNA has been regarded as one of the essential ways for regulating plant growth, development, and immunity (Tang and Chu, 2017).

In rice, over 700 mature miRNAs have been identified in the genome (Tang and Chu, 2017) and at least 70 miRNAs respond to *Magnaporthe oryzae* (M. oryzae) infection, meaning that many miRNAs are involved in rice immunity (Li et al., 2014). Among them, 16 miRNAs have been characterized as fine regulators affecting rice blast resistance (Feng et al., 2021; Wang et al., 2021), as positive regulators, such as Osa-miR1320, Osa-miR160a, Osa-miR162a, Osa-miR166k-h, Osa-miR398b, and Osa-miR7695 (Li et al., 2014; Li, Jeyakumar, et al., 2019b; Quoc et al., 2019; Salvador-Guirao et al., 2018; Sánchez-Sanuy et al., 2019; Wang et al., 2021), or as negative regulators, such as Osa-miR156, Osa-miR164a, Osa-miR167d, Osa-miR168, Osa-miR169a, Osa-miR319b, Osa-miR396, Osa-miR444b.2,

Osa-miR1873, and Osa-miR535 (Chandran et al., 2019; Li et al., 2017; Wang et al., 2016, 2018, 2021; Zhang et al., 2018, 2020; Zhao et al., 2019; Zhou et al., 2019). Further investigation revealed that Osa-miR535 targets the *SQUAMOSA Promoter Binding Protein Like 14* (*OsSPL14*) (Wang et al., 2021). *OsSPL14* is also known as *Ideal Plant Architecture 1* (*IPA1*), which promotes grain yield and blast resistance via boosting the expression of downstream transcription factor genes *DEP1* and *WRKY45*, respectively (Jiao et al., 2010; Miura et al., 2010; Shimono et al., 2007). Consistently, over-expressing Osa-miR535 (OX535) results in compromised rice blast resistance accompanied by less filled grains, smaller panicles, and more tillers compared to wild-type (WT), indicating that the Osa-miR535-*OsSPL14* module acts in the coordination of growth, development, and immunity (Wang et al., 2021).

The mature sequences of Osa-miR535 share high similarity with Osa-miR156 and Osa-miR529, although they are derived from different *MIR* genes (Sun et al., 2019; Wang et al., 2021). They target the same transcription factor gene family of *SPL* that is comprised of 19 members in rice to regulate plant growth and immunity (Sun et al., 2019; Xie et al., 2006; Wang et al., 2015; Zhang et al., 2020). *OsSPL7*, *OsSPL14*, and *OsSPL17* are fine-tuned by Osa-miR156 and Osa-miR529 for an optimal panicle size of rice (Wang et al., 2015; Yue et al., 2017). In addition, Osa-miR535 is highly expressed in panicles, which leads to the suppression of *SPL* genes, including *OsSPL7*, *OsSPL12*, *OsSPL14*, and *OsSPL16* (Sun et al., 2019; Wang et al., 2021). Osa-miR156 has been identified as a negative regulator in rice immunity against *M. oryzae* infection (Zhang et al., 2020). Over-expressing Osa-miR156 enhances the susceptibility to blast disease in rice. Conversely, over-expressing a target mimic of Osa-miR156 (MIM156) confers higher resistance compared to WT. Further investigation revealed that Osa-miR156 specifically targets the *OsSPL14* gene and downregulates its expression resulting in compromised blast resistance (Zhang et al., 2020). In addition, Osa-miR156 targets *OsSPL7* to regulate rice resistance to *Xanthomonas oryzae* pv. *oryzae* (*Xoo*) (Liu et al., 2019). However, it is unclear whether Osa-miR535 targets the other *SPL* genes to regulate rice immunity.

In the present study, based on the expression pattern of *SPL* genes in WT, OX535 and MIM535, we identified that *OsSPL4* is another target of Osa-miR535 and necessary for rice blast resistance. Further investigation of the mechanism identified the pathway of *OsSPL4-GH3.2* paralleling the *OsSPL14-WRKY45* module regulated by Osa-miR535 in rice immunity.

RESULTS

Osa-miR535 negatively regulates rice immune responses

In a previous study, transcription analysis revealed that Osa-miR535 is one of the miRNAs responsive to the infection of *M. oryzae* in both the susceptibility accession Lijiang xin Tuan Heigu (LTH) and the resistance accession International Rice Blast Line Pyricularia-Kanto51-m-Tsuyuake (IRBLkm-Ts) (Li et al., 2014). Here, the expression pattern of Osa-miR535 was further investigated by a quantitative polymerase chain reaction with reverse transcription (RT-PCR), which confirmed that Osa-miR535 was induced by *M. oryzae* infection in LTH at 12 and 48 h post inoculation (h.p.i.) compared to mock treatment. However, it was suppressed in IRBLkm-Ts (Figure S1a). Intriguingly, the Osa-miR535 level was significantly suppressed at the early stage upon chitin treatment in both LTH and IRBLkm-Ts, although its expression was still higher in LTH than that in IRBLkm-Ts (Figure S1b), indicating that miR535 may be involved in rice immunity. To confirm this hypothesis, we generated the transgenic lines overexpressing Osa-miR535 (OX535) and expressing a target mimic of Osa-miR535 (MIM535) (Figure S2), respectively. The even mixture of *M. oryzae* strains GZ8, a GFP-tagged strain Zhong 8-10-14, and 97-27-2 were used for the disease assay via spraying inoculation. Compared with WT, OX535 lines showed more susceptibility; by contrast, MIM535 lines enhanced the resistance (Figure 1a,b), suggesting that Osa-miR535 negatively regulates rice blast resistance. This is consistent with the conclusion obtained from pouching inculcation in a recent study (Wang et al., 2021).

To investigate how Osa-miR535 affects rice immunity, we examined the expression of defense-related marker genes, *pathogenesis-related gene 1a* (*PR1a*) and *ENT-KAURENE synthase 4* (*KS4*), in WT, OX535, and MIM535 lines upon *M. oryzae* strain GZ8 infection (Park et al., 2012; Zhang et al., 2015). *PR1a* and *KS4* were significantly induced by *M. oryzae* in all lines. Compared with WT, the induction was enhanced in MIM535 lines but suppressed in OX535 lines at 48 h.p.i. (Figure 1c). In addition, the *KS4* gene was significantly induced at 6 h post chitin treatment (hpt) in both WT and MIM535 lines (Figure S3a). The *NAC-domain-containing protein 4* (*NAC4*), an earlier induced basal defense-related gene (Park et al., 2012), was also significantly upregulated in both WT and MIM535 begin at 1 hpt, which achieved a peak at 3 hpt, and then was reduced at 6 hpt. The induction of *NAC4* was higher in MIM535 lines than that in WT at 1 and 3 hpt (Figure S3b). These data suggest that Osa-miR535 negatively regulates the defense-related genes at the early stage of *M. oryzae* infection.

Next, we examined the pathogenesis of *M. oryzae* strain GZ8 expressing a GFP in the sheath cells. Compared with WT, the GZ8 grown faster in OX535 but slower in MIM535 at both 24 and 48 h.p.i. (Figure 1d). Statistically, although approximately 40% germinated spores formed the invasive hyphae in the local cell (the first cell), 3% extended into the neighbor cells (the second cells) in WT at 24 h.p.i. Over

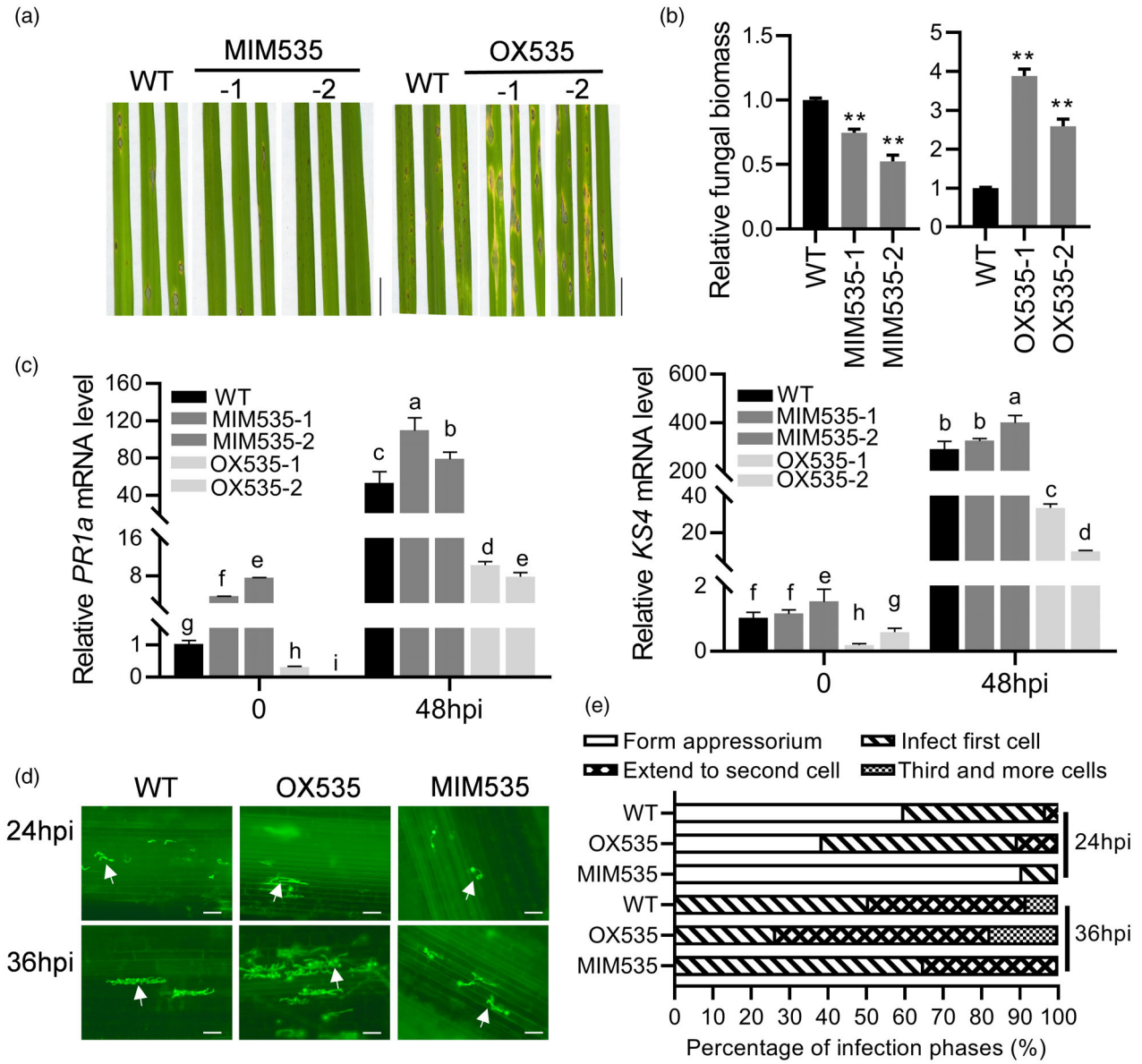

Figure 1. Osa-miR535 negatively regulates rice immunity against *Magnaporthe oryzae*. (a) The disease phenotype was recorded at 5 d.p.i. *M. oryzae* strains GZ8 and 97-27-2 were evenly mixed for examining the phenotypes of MIM535 and OX535 by spray inoculation. Scale bars = 1 cm. (b) Quantified relative fungal biomass by measuring *MoPot2* gene against *OsUbiquitin* DNA level. Error bars indicate the SD ($n = 3$). A double asterisk (**) indicates a significant difference ($P < 0.01$) via Student's *t* test compared to WT. (c) The expression of defense-related genes *PR1a* and *KS4* in WT, OX535, and MIM535 lines at the early stage of *M. oryzae* infection. Error bars indicate the SD ($n = 3$). Different letters above the bars indicate a significant difference ($P < 0.05$), as determined by one-way ANOVA followed by post-hoc Tukey's honestly significant difference analysis. (d) Infection process of *M. oryzae*. Representative images were taken at 24 and 36 h.p.i. to record the growth of *M. oryzae* strain GZ8 in sheath cells of the indicated lines. Arrows indicate an invasive hyphal. Scale bars = 10 μm. (e) The quantified infection process of *M. oryzae*. More than 200 germinated conidia in each line were analyzed. These experiments were repeated twice with similar results being obtained.

60% hyphae invaded in the first cell and 10% of them already grew in the second cells in OX535, although only 10% invaded in the first cell without second cell invasion in MIM535 (Figure 1e). This trend of GZ8 strain grown in different lines was continued at 48 h.p.i. Over 8% of hyphae extended into the neighbor cells of the second cells (the third cells or more) in WT, and 16% occurred in OX535, although no third or more cells invasion occurred in MIM535 (Figure 1e). Simultaneously, we examined H_2O_2 accumulation at 48 h.p.i. and found that the infected cells were stained darker brown in MIM535, but lighter in OX535, compared to WT (Figure S4). These results indicate that Osa-miR535 facilitates *M. oryzae* invasion and suppresses H_2O_2 accumulation at the early infection stage.

The expression of several *SPL* genes is affected by Osa-miR535

For screening the target genes of Osa-miR535, the miRNA target prediction online tool, psRNATarget website (http://plantgrn.noble.org/psRNATarget), was used and predicted 14 potential targets with strict parameters. Among them, 12 potential target genes were members of the *SPL* gene family, including *OsSPL2*, *3*, *4*, *7*, *11*, *12*, *13*, *14*, *16*, *17*, *18*, and *19*. Several *SPL* genes have been identified as targets of Osa-miR156 and Osa-miR529 that show high conservation with Osa-miR535 in the amino acid sequence (Figure S5) (Wang et al., 2015; Xie et al., 2006; Yue et al., 2017). *OsSPL14* has been identified as the target of Osa-miR535 (Wang et al., 2021). Therefore, we examined the expression of these *SPL* genes, except *OsSPL14*, in WT, MIM535, and OX535, and found that the expression of *OsSPL3*, *4*, *7*, *11*, *12*, and *16* was largely decreased in OX535 lines and increased in MIM535 lines (Figure 2a). Among them, the expression of *OsSPL4* was affected the greatest by Osa-miR535. Therefore, we further investigated whether *OsSPL4* is another *SPL* gene targeted and negatively regulated by Osa-miR535.

OsSPL4 gene is targeted by Osa-miR535

It is well known that plant miRNAs are highly complementary to their binding sites in target genes for regulating the mRNA level by cleavage or inhibiting translation (Rogers and Chen, 2013; Sanei and Chen, 2015). Therefore, a reporter assay was used to investigate whether mRNA of *OsSPL4* was negatively regulated by Osa-miR535. We made a construct expressing YFP fused with the predicted binding site of Osa-miR535 in *OsSPL4* ($SPL4_{TBS}$) at the N-terminus (*$SPL4_{TBS}$-YFP*) and used it in the reporter system co-expressing with or without *35S::miR535*. The highest YFP intensity was in the region transient-expressing *$SPL4_{TBS}$-YFP* alone, whereas YFP intensity was decreased as a result of the rise Osa-miR535 in co-expression. However, this trend was not observed in the control co-expressing YFP and Osa-miR535 (Figure 2b). This observation suggested that Osa-miR535 binds on the predicted site of *OsSPL4* and suppresses the expression of the fusion gene. We mapped the directed cleavage sit of Osa-miR535 in *OsSPL4* mRNA using the 5′ RNA ligase-mediated rapid amplification of cDNA ends (5′ RLM-RACE) technique in OX535 plants. The results revealed that cleavage occurred between the 10th and 11th base pair in the predicted Osa-miR535 binding site in the 3′ untranslated region of *OsSPL4* (Figure 2c), indicating that *OsSPL4* can be precisely cleaved *in vivo* by Osa-miR535. All of these data suggest that *OsSPL4* is an authentic target gene and is directly cleaved by Osa-miR535 for negatively regulating its expression.

OsSPL4 enhances rice blast disease resistance

To further investigate whether *OsSPL4* is involved in Osa-miR535-mediated rice blast susceptibility, we examined *OsSPL4* expression in Nipponbare leaves and found that it was significantly induced by *M. oryzae* inoculation (Figure 3a). Therefore, we made transgenic plants with overexpressed *OsSPL4* (OXSPL4) and knocked out *OsSPL4* (*osspl4* mutant) via CRISPR (clustered regularly interspaced short palindromic repeats)/Cas9 gene-editing

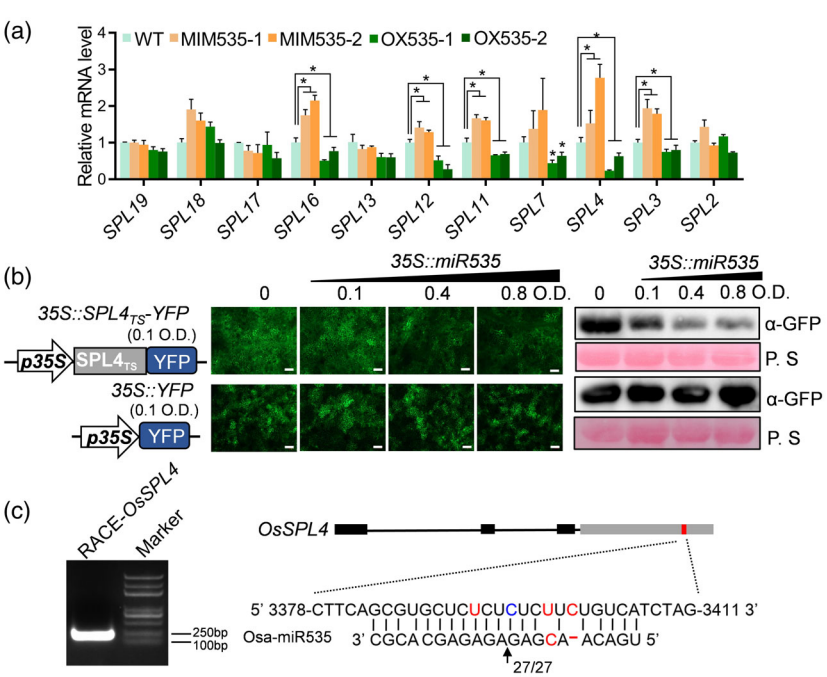

Figure 2. *OsSPL4* is the target gene of Osa-miR535. (a) The expression of *SPL* family genes in WT, OX535, and MIM535 transgenic plants. Four-week-old seedlings were examined for gene expression by RT-qPCR. Error bars indicate the SD ($n = 3$). An asterisk (*) indicates a significant difference ($P < 0.05$) via Student's *t* test. (b) Osa-miR535 suppressed the expression of *$SPL4_{TBS}$-YFP*. Two samples of agrobacteria respectively harbored the construct expressing *35S::miR535* and *35S::$SPL4_{TBS}$-YFP*, and mixed with a different ratio for co-expressing in *Nicotiana benthamiana*. The confocal images were taken 36 h after infiltration. Scale bar = 50 μm. Simultaneously, the protein level of $SPL4_{TBS}$-YFP and YFP was detected by anti-GFP sera. The total protein was stained by Ponceau S (P. S) as a loading control. (c) The Osa-miR535 cleavage site in *OsSPL4* mRNA was identified by 5′ RLM-RACE. Twenty-seven clones were randomly selected for sequencing. A black arrow indicates the cleavage site.

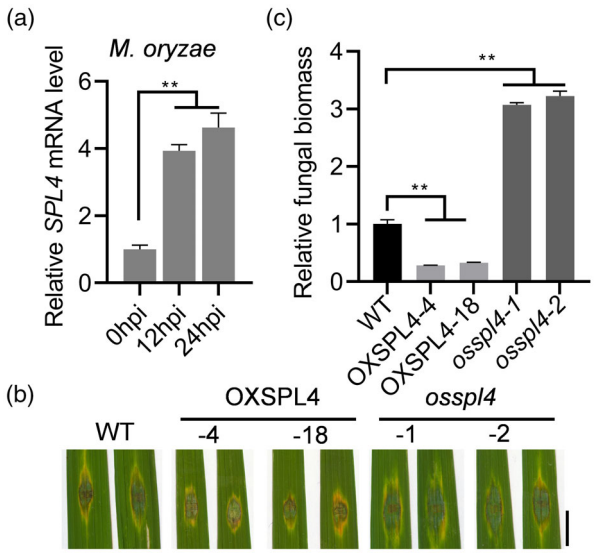

Figure 3. OsSPL4 enhances rice resistance to Magnaporthe oryzae. (a) The expression of OsSPL4 was induced by M. oryzae in 4-week-old seedlings of Nipponbare. (b) OsSPL4 enhanced rice blast disease resistance. The representative disease phenotype was recorded at 5 d.p.i. for the M. oryzae strain GZ8 by punch-inoculation. Scale bars = 5 mm. (c) Quantified relative fungal biomass from (b). Error bars indicate the SD (n = 3). A double asterisk (**) indicates a significant difference ($P < 0.01$) via Student's t test compared to WT. These experiments were repeated twice with similar results being obtained.

technology. We obtained 18 overexpression transgenic lines. Lines 4 and 18 showed a more than 10-fold increased expression of *OsSPL4* (Figure S6). Two *osspl4* mutants, *osspl4-1* and *osspl4-2*, had a C insertion and deletion in the guide RNA region at the N-terminal of *OsSPL4*, respectively, leading to frame shift mutations with an early stop codon (Figure S7). Next, these transgenic lines and mutants were subjected to rice blast resistance analysis at the seedling stage together with WT. Compared with WT, the OXSPL4-4 and -18 displayed smaller disease lesions with less fungal biomass, although *osspl4-1* and *-2* mutants showed reverse phenotypes (Figure 3b,c). These results indicate that *OsSPL4* positively regulates rice blast disease resistance.

OsSPL4 enhances rice immune responses and delays *M. oryzae* infection

To further investigate *OsSPL4* regulated rice immunity against *M. oryzae*, we examined the expression of defense-related marker genes in WT, OXSPL4, and *osspl4* mutant. Upon inoculation of *M. oryzae* strain GZ8, the expression of *PR1a* and *KS4* was significantly upregulated in OXSPL4 compared to the control plants at 12 and 24 h.p.i. By contrast, *PR1a* and *KS4* were downregulated in *osspl4* mutant at 12 h.p.i. (Figure 4a), indicating that *OsSPL4* positively regulates the expression of defense-related genes. In addition, we examined the pathogenesis of *M. oryzae* and the accumulation of H_2O_2 in the infection process in rice sheath cells. The *M. oryzae* strain GZ8 grew faster in the sheath cells of *osspl4* mutant than WT at 24 h.p.i., although growth was slower in OXSPL4 (Figure 4b). Statistically, 12.5% of germinated spores formed invasive hyphae in the first cell in WT, and over 61% occurred in *osspl4* mutant. However, all germinated spores stayed in the appressorium formation stage in OXSPL4 (Figure 4c). This difference increased further at 36 h.p.i., with all germinated spores infecting the first cells and 20% extending to second cells in WT. However, the *M. oryzae* grew faster in *osspl4* mutant, with 35% extending to second cells and 13% extending to the third or more cells. By contrast, most of the invasive hyphae were hampered in the first infected cell and none extended to the second cell in OXSPL4 (Figure 4c). These results indicate that *OsSPL4* hampers the *M. oryzae* invasion process. Meanwhile, we examined H_2O_2 accumulation using 3,3′-diaminobenzidine (DAB) staining. Compared with WT, the infected sheath cells of OXSPL4 were stained dark brown, although little brown was observed in *osspl4* mutant (Figure 4d), which suggests that *OsSPL4* promotes H_2O_2 accumulation in the infected process of *M. oryzae*.

OsSPL4 localizes in the nucleus and exists ubiquitously in different rice tissues

To further investigate the function of *OsSPL4*, we first characterized the subcellular localization and expression pattern of *OsSPL4*. Bioinformatics analysis indicated that *OsSPL4* has a putative nuclear localization signal. To validate the localization of *OsSPL4*, we fused *OsSPL4* to the N-terminal of *YFP* (*35S::SPL4-YFP*), followed by co-expression with the construct expressing *35S::RFP-NLS*, a nuclear marker, in *Nicotiana benthamiana*. Subcellular localization analysis showed that SPL4-YFP fusion protein localizes in the nucleus (Figure 5a).

RT-qPCR was employed to investigate the temporal and spatial expression pattern of *OsSPL4*. *OsSPL4* had the highest expression level in the young panicle and maintained a higher expression in root, leaf, and culm, but a low expression in flowers and coleoptile (Figure 5b). These data suggested that *OsSPL4* is widely expressed in different organs of rice, but with a bias in panicle, leaf, and root. In addition, we also investigated *OsSPL14*, a homologue gene of *OsSPL4* involved in rice immunity, and their cognate miRNAs, Osa-miR535 and Osa-miR156. Osa-miR535 is highly expressed in flower, and Osa-miR156 and *OsSPL4* are expressed to a lower extent in leaf and culm (Figure 5b), indicating the spatiotemporal difference between these two miRNAs and *SPLs*.

OsSPL4 protein directly binds the promoter of *GH3.2* and enhances its expression

SPL genes encode a class of plant-specific transcription factors that have important roles in development and

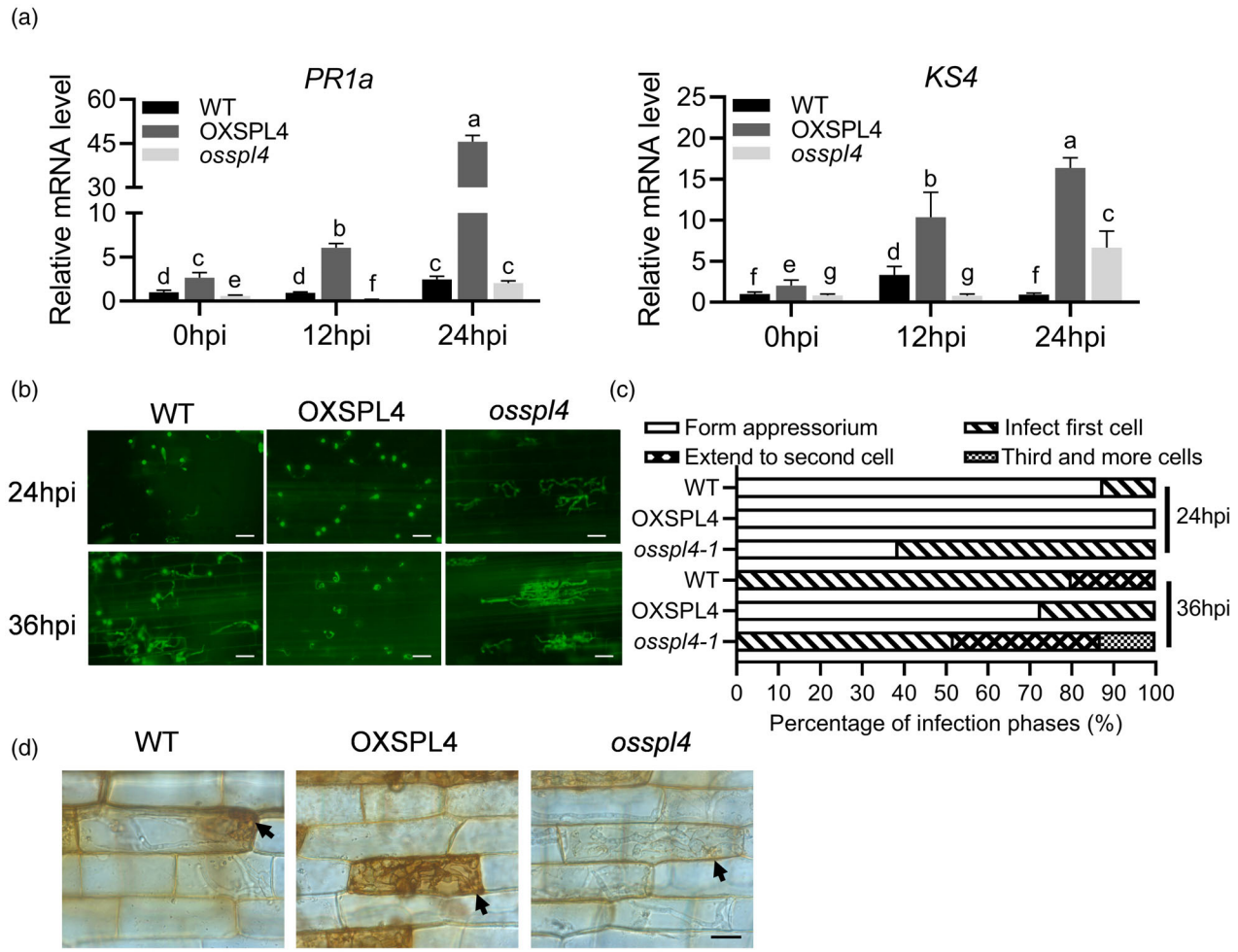

Figure 4. *OsSPL4* enhances the immune response against *Magnaporthe oryzae* infection. (a) *OsSPL4* enhanced the expression of defense-related genes. Four-week-old seedlings of WT, OXSPL4, and *osspl4* were used to examine gene expression at the indicated time points after *M. oryzae* strain GZ8 inoculation. Error bars indicate the SD ($n = 3$). Different letters above the bars indicate a significant difference ($P < 0.05$), as determined by one-way ANOVA analysis followed by post-hoc Tukey's honestly significant difference analysis. (b) *OsSPL4* blocked the infection process of *M. oryzae*. The representative images record the growth of *M. oryzae* strain GZ8 at 24 and 36 h.p.i. in sheath cells. Scale bars = 10 μm. (c) Statistical analyses of *M. oryzae* growth. More than 200 conidia were analyzed in each line. (d) *OsSPL4* enhanced H_2O_2 accumulation in *M. oryzae* infection. The leaf sheathes of the indicated lines were subjected to DAB staining at 48 h.p.i. Arrows indicate an invasive hyphal. Scale bars = 10 μm. These experiments were repeated twice with similar results being obtained.

immunity in Arabidopsis and rice (Birkenbihl et al., 2005; Cardon et al., 1999; Liu et al., 2019; Wang et al., 2018). To further identify the downstream component regulated by Osa-miR535-*OsSPL4* module, we performed the prediction for screening the binding targets of OsSPL4 via the online tool PLACE (https://www.dna.affrc.go.jp/PLACE) and found that *GH3.2* is one of the candidate genes. *GH3.2* encodes an indole-3-acetic acid (IAA)-amido synthetase, which acts in IAA homeostasis and enhances rice immunity against *M. oryzae* (Fu et al., 2011). In addition, bioinformatic analysis revealed that there are several GTAC motifs in the *GH3.2* promoter (Figure S8). The GTAC motif was reported as a site recognized and bonding specifically by the SQUA promoter-binding (SBP)-domain of SPL proteins (Birkenbihl et al., 2005). We first examined the *GH3.2* expression pattern in LTH and IRBLkm-Ts upon *M. oryzae* inoculation. The expression of *GH3.2* was significantly induced in both LTH and IRBLkm-Ts at 12 and 24 h.p.i., and it was always expressed to a greater extent in IRBLkm-Ts compared to LTH (Figure 6a). In addition, *GH3.2* was significantly upregulated in both MIM535 and OXSPL4 compared to WT (Figure 6b). Other *GH3* members did not show an apparent difference in WT, OXSPL4, and *osspl4* (Figure S9). These data suggest that the *GH3.2* might function downstream of *OsSPL4*.

To further investigate whether OsSPL4 bind to the *GH3.2* promoter, we used a yeast-one-hybrid (Y1H) assay and a Dual-Luciferase Reporter Gene Assay Kit (Beyotime, Shanghai, China) to assess the binding stability of OsSPL4 protein on the *GH3.2* promoter. As shown in Figure 6c,

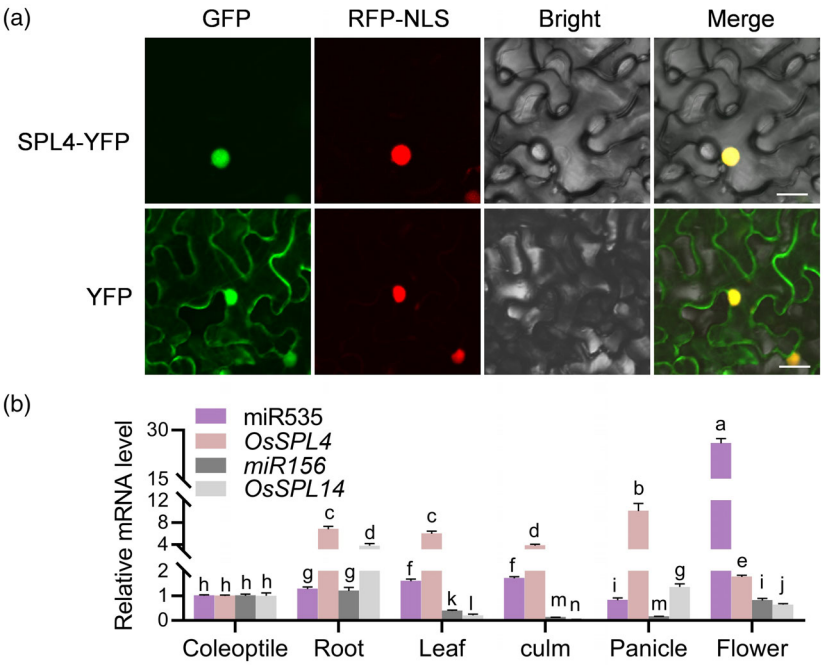

Figure 5. Subcellular localization and expression profile of *OsSPL4*. (a) Confocal images show the subcellular localization of SPL4-YFP in the nucleus. *35S::SPL4-YFP* and *35S::YFP* were, respectively, co-expressed with *35S::2* × *RFP-NLS* in *Nicotiana benthamiana* leaves. *35S::2* × *RFP-NLS* was used as the nuclear marker. (b) The expression of Osa-miR535, *OsSPL4*, Osa-miR156, and *OsSPL14* in the indicated tissues of Nipponbare. Coleoptile was collected 2 days after seed germination. Root, leaf, and culm were collected 40 days after seeding. Different letters above the bars indicate a significant difference ($P < 0.05$), as determined by one-way ANOVA analysis followed by post-hoc Tukey's honestly significant difference analysis.

OsSPL4 could bind to the *GH3.2* promoter in yeast cells. Moreover, *OsSPL4* was identified to enhance the expression of the luciferase gene that was expressed by the *GH3.2* promoter in *N. benthamiana* (Figure 6d). However, the binding was disrupted in the mutated OsSPL4 protein that lacked its C-terminal containing the SBP domain ($SPL4_{\Delta C}$) or the mutated *GH3.2* promoter missing the GTAC core motif (GH3.2 m) (Figure 6c), indicating that OsSPL4 binds to the *GH3.2* promoter, which is dependent on the recognition between the SBP domain and the GTAC motif.

Then, we performed an electrophoretic mobility shift assay (EMSA) to investigate the direct recognition between OsSPL4 and the *GH3.2* promoter. The SBP domain of OsSPL4 was fused with GST at the N-terminal (GST-$SPL4_{SBP}$) and the fusion protein was expressed and purified from prokaryotic protein expression system. The EMSA showed that GST-$SPL4_{SBP}$ bound to the probe covering GTAC core motifs of the GH3.2 promoter (Figure 6e). Such binding was largely blocked by the unlabeled GH3.2 pro, but not by mutated GH3.2 promoter, which lacked a GTAC motif (GH3.2 pro-mutant) (Figure 6e), indicating that the GTAC motif in the GH3.2 promoter is essential for OsSPL4 binding. Intriguingly, OsSPL4 could not bind to the WRKY45 promoter that was bonded by OsSPL14 (Figure 6e), although it positively regulated the expression of *WRKY45* (Figure S10).

The *EXPA* genes encode cell wall-loosening expansin proteins, resulting in the cell wall (i.e. the physical barrier of plant cell) being vulnerable to pathogens (Ding et al., 2008; Fu et al., 2011). The *EXPA* genes are downstream components of the IAA signal pathway and negatively regulated by *GH3.2* (Fu et al., 2011). Therefore, we considered whether the *EXPA* genes are regulated by *OsSPL4* that functions upstream of *GH3.2*. The expression of *EXPA* family genes was investigated in *OsSPL4* transgenic lines, and *EXPA1* and *EXPA5* were significantly decreased in OXSPL4 lines with increasing *GH3.2* (Figure 6b and Figure S11). In conclusion, these data suggest that *GH3.2* is regulated by *OsSPL4*, in parallel with the *OsSPL14-WRKY45* module targeted by Osa-miR535 for regulating rice immunity against *M. oryzae* (Figure 7).

DISCUSSION

miRNA-mediated gene silencing plays a vital role in plant immunity against pathogen infection. Several miRNAs are reported to act positively or negatively in rice immunity (Li, Jeyakumar, et al., 2019b). Osa-miR535 has been identified to compromise rice blast resistance by suppressing the expression of *OsSPL14* gene (Wang et al., 2018). In the present study, we found that Osa-miR535 also suppresses *OsSPL4*, which in turn regulates the expression of G*H3.2*, a key regulator for immunity and IAA homeostasis (Figure 7). Our discovery highlights that Osa-miR535 employs two *SPL* genes to manipulate, in parallel, rice immunity against *M. oryzae*.

SPL family genes encode plant-specific transcription factors (Hua et al., 2019) that bind with the DNA sequence carrying a GTAC core motif via their conserved SBP domain (Birkenbihl et al., 2005). In Arabidopsis, SPL7 binds to the GTAC motif in the promoter of miR398, which was reported to elevate the expression of miR398 and downregulate the expression of copper/zinc superoxide

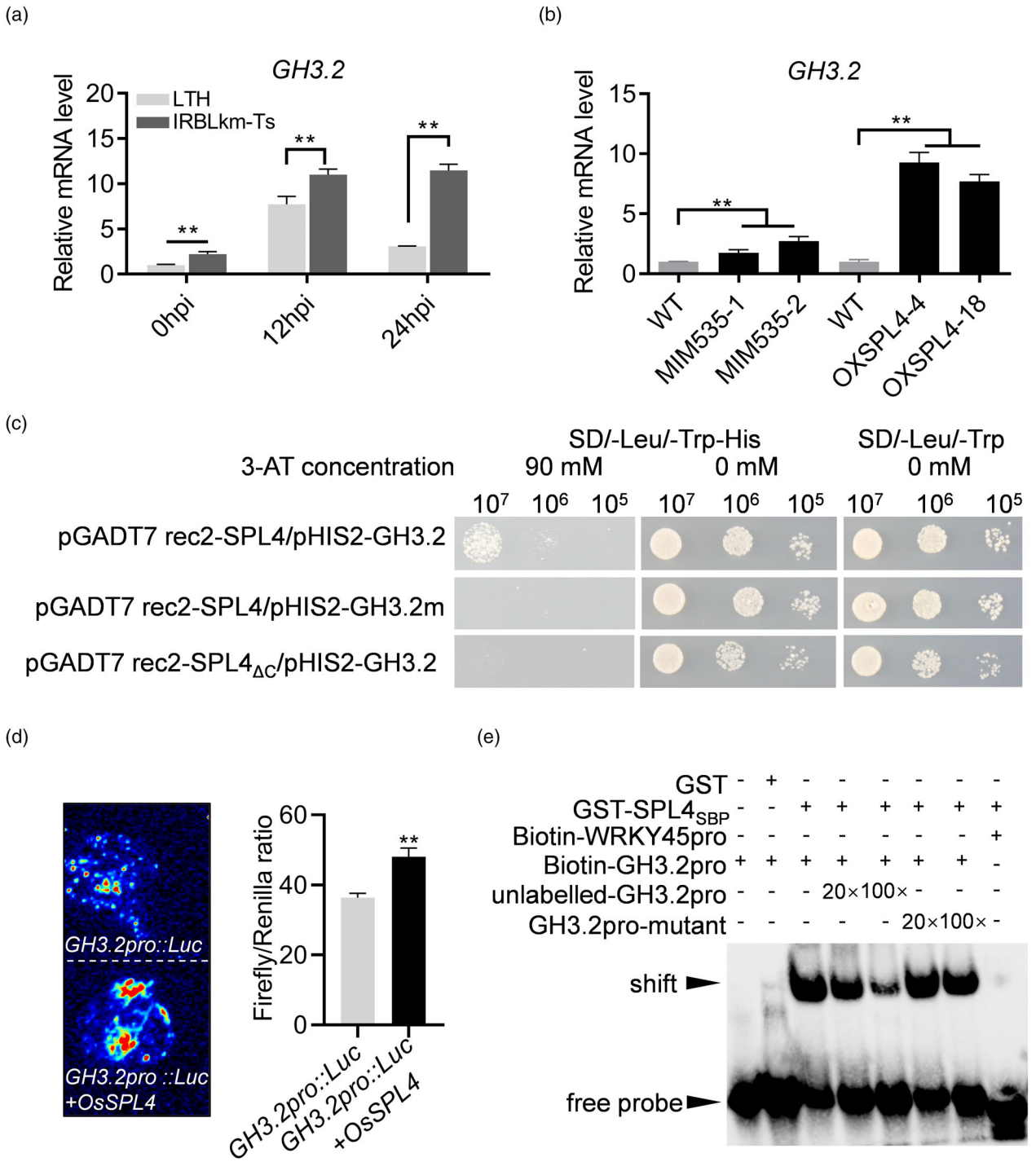

Figure 6. OsSPL4 binds to the promoter of GH3.2 to regulate its expression (a) The expression of GH3.2 was induced by Magnaporthe oryzae infection in LTH and IRBLkm-Ts. (b) The expression of GH3.2 was enhanced in MIM535 and OXSPL4. (c) OsSPL4 binds to the GH3.2 promoter in a Y1H assay. (d) OsSPL4 enhanced the activity of the GH3.2 promoter in the dual-LUC assay. The Firefly/Renilla ratio indicates the relative luciferase activity. Error bars indicate the SD (n = 3). A double asterisk (**) indicates a significant difference ($P < 0.01$) via Student's t test compared to the control. (e) SBP domain of OsSPL4 binds to the region harboring GTAC motif in the GH3.2 promoter in EMSA assay.

dismutase in copper deficiency conditions (Yamasaki et al., 2009). In rice, OsSPL14 binds the GTAC motif in the promoter of *DEP1* to regulate tiller development. In the present study, we used this theory to predict the candidate target genes of SPL4. It is fast and specific with respect to identifying that OsSPL4 binds the GTAC motif in the

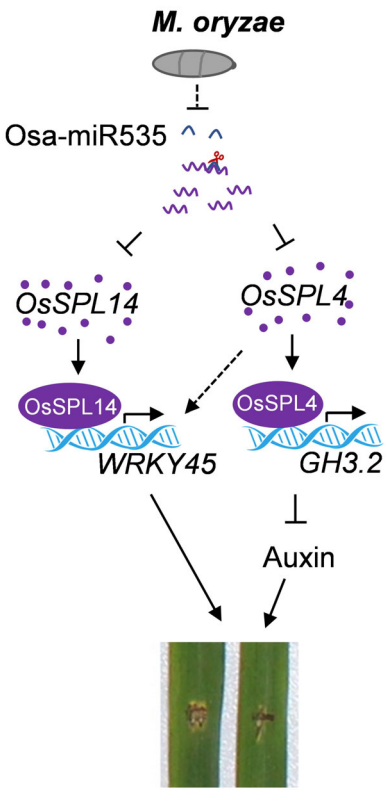

Figure 7. A working model for Osa-miR535 -*OsSPL4-GH3.2* module in rice immunity *OsSPL4* is one of target genes of Osa-miR535. OsSPL4 protein binds to the GTAC motif in the *GH3.2* promoter via its SPB domain. GH3.2 is an IAA-amido synthetase that catalyzes free IAA to IAA-amino acid as an inactive form to suppress IAA signaling. Upon *Magnaporthe oryzae* infection, Osa-miR535 is suppressed, which releases the suppression of *OsSPL4* by Osa-miR535. The increased OsSPL4 promotes the expression of *GH3.2*, which breaks the homeostasis of IAA, causing a decrease in free IAA. Subsequently, the IAA signal pathway is finally suppressed to enhance rice blast resistance.

promoter of *GH3.2* and enhances its expression (Figure 6c–e), suggesting the GTAC motif is a key pointer for finding out the target genes of SPL family proteins.

GH3.2 has been identified to confer broad-spectrum resistance to pathogens of bacterial blight and fungal blast. Its expression is induced by *M. oryzae* infection. Overexpressing *GH3.2* enhanced (but suppressing it via RNAi reduced) the resistance to rice blast (Fu et al., 2011). *GH3.2* encodes an IAA-amido synthetase to affect IAA homeostasis, which catalyzes free IAA conjugating with amino acids in the storage pool. It is still unknown whether the IAA homeostasis affected by *GH3.2* is only a biological phenomenon or is also the reason for *GH3.2* mediated rice immunity. Some studies have identified that IAA biosynthesized by pathogens or plants can facilitate pathogenesis with compromised plant immune responses (Naseem et al., 2015). The extent of, or the increase, in plant immunity modulated by IAA remains inknown. Intriguingly, IAA-ASP treatment increases the pathogen progress of *Botrytis cinerea* and *Pst DC3000* in Arabidopsis (González-Lamothe et al., 2012), suggesting that IAA-ASP negatively regulates plant immunity. Nevertheless, overexpressing *GH3.2* enhances rice blast resistance accompanied by increased IAA-ASP, suggesting that IAA homeostasis may simply be a biological phenomenon. *GH3.2* could employ another pathway, such as increased expansins (Figure 3b and Figure S11), but not IAA homeostasis to boost rice immunity against *M. oryzae*. Therefore, further studies are required to dissect the *GH3.2* conferred plant immunity and finally reveal the mechanism underlying Osa-miR535-*SPL4-GH3.2* module mediated rice blast resistance.

Osa-miR535 has been characterized as targeting *OsSPL14* for regulating rice immunity against *M. oryzae* positively (Zhang et al., 2020; Wang et al., 2021). The emerging evidence supports the idea that one miRNA may target different genes to perform its function redundantly. Accordingly, Osa-miR535 downregulates *OsSPL7*, *OsSPL12*, and *OsSPL16* in panicles (Sun et al., 2019). Consequently, we further screened the target gene of Osa-miR535 in the *SPL* gene family. As expected, we successfully identified that *OsSPL4* is targeted by Osa-miR535, as well as its homologous gene *OsSPL14*, to fine-tune rice immunity against *M. oryzae* (Figure 7). OsSPL14 binds on the promoter of *WRKY45* to boost its expression for enhancing rice blast resistance (Wang et al., 2018). In the present study, OsSPL4 binds on the promoter of *GH3.2* (Figure 6), which acts in IAA homeostasis and enhances rice immunity against *M. oryzae* (Fu et al., 2011), suggesting that Os-miR535 targets two parallel pathways of *SPL14-WRKY45* and *SPL4-GH3.2* to manipulate rice blast resistance. In addition, OsSPL4 also promotes the expression of *WRKY45* (Figure S10), even though it cannot bind with the promoter of *WRKY45*, similar to OsSPL14 (Figure 6e), indicating that it may exist cooperatively downstream of *SPL* genes to regulate plant immunity. Upstream of *SPL* genes, *OsSPL14* is also targeted by Os-miR156 and Osa-miR535 to control rice immunity (Zhang et al., 2020; Wang et al., 2021). Moreover, *OsSPL7* is targeted by Osa-miR156, Osa-miR529, and Osa-miR535, three highly conserved miRNAs (Figure S2) (Sun et al., 2019; Wang et al., 2015; Yue et al., 2017). *OsSPL14* and *OsSPL17* are target genes of Osa-miR156 and Osa-miR529 (Wang et al., 2015; Yue et al., 2017). These data suggest that there may be a complex regulatory network consisting of the three miRNAs (Osa-miR535, Osa-miR156, and Osa-miR529) and *SPL* genes to modulate immunity in rice. Furthermore, Osa-miR156 targets *OsSPL14* to define the ideal plant architecture (Jiao et al., 2010; Miura et al., 2010) and targets *OsSPL3* to regulate crown root development and cold tolerance (Shao et al., 2019; Zhou and Tang, 2018). Osa-miR529 spatiotemporally regulates *OsSPL2*, *OsSPL7*, *OsSPL14*, *OsSPL16*, *OsSPL17*, and *OsSPL18* in different life

stages to control several important agronomic traits, including plant height, tiller number, panicle architecture, and grain size (Yan et al., 2021). Therefore, this complex network may be extensively involved in rice growth and abiotic stresses.

Spatio-temporal expression is an important feature of these three miRNAs and *SPL* genes. Osa-miR529 is ubiquitously expressed in leaf, root, and panicle, but more preferentially in panicle (Jeong et al., 2011). Osa-miR156 can be detected in coleoptile, root, leaf, culm, panicle, and flower, although its expression is low in leaf, culm, and panicle (Figure 5b). Compared with Osa-miR156, Osa-miR535 is ubiquitously expressed in all of these tissues and more preferentially in flower (Figure 5b). *OsSPL14* is remarkably expressed in panicle but rarely detected in leaf tissue (Figure 5b) (Wang et al., 2015). In addition, *OsSPL4* has a higher expression than *OsSPL14* in leaf and panicle (Figure 5b). However, *OsSPL14* and *OsSPL4* are required for rice blast resistance in leaves (Figure 3) (Wang et al., 2015). Taken together, those findings provide a research foundation for dissecting the mechanisms underlying the network consisting of Osa-miR156, Osa-miR529, and Osa-miR535, as well as their targeted *SPL* genes, in rice growth, development, and immunity.

EXPERIMENTAL PROCEDURES

Plant materials and growth conditions

The rice (*Oryza sativa*) accessions used in the present study included the susceptible accession Lijiangxin tuan Heigu (LTH) and International Rice Blast Line Pyricularia-Kanto 51-m-Tsuyuake (IRBLkm-Ts) (Lin et al., 2001; Tsunematsu et al., 2000). Nipponbare was used as WT to generate transgenic plants. All rice plants were grown in the greenhouse under a 14:10 h light/dark photocycle and 70% relative humidity at 26°C. *Nicotiana benthamiana* was planted in the greenhouse under a 16:8 h light/dark photocycle at 24°C.

Genetic transformation plasmid construct and mutant screening

To generate transgenic plants expressing artificial target mimic of Osa-miR535, target mimicry sequences of Osa-miR535-5p were used to replace the miR399 target site in *IPS1* by PCR application with primers miR535-IPS1-F/R and miR535 mimic-F/R as described previously (Franco-Zorrilla et al., 2007; Wang et al., 2021) and were then cloned into the *Kpn*I–*Bcu*I sites of the binary vector *pCAMBIA1300-35S* with hygromycin selection (Table S1). To achieve overexpression of Osa-miR535 transgenic plants, a fragment containing 431 bp upstream and 495 bp downstream of Osa-miR535 was amplified from Nipponbare with primers OXmiR535-F/R (Table S1). The fragment was cloned into the *Kpn*I–*Sal*I sites of the binary vector *pCAMBIA1300-35S*, resulting in the construct *p35S::MIR535*. For *OsSPL4* overexpression lines, the coding sequence of *OsSPL4* was cloned into pCAMBIA1300 vector by *Kpn*I-*Sal*I sites to generate the *pCAMBIA1300-SPL4* with primers OXSPL4-F/R (Table S1). To knockout *OsSPL4* gene via CRISPR/Cas9 genome editing technology, two gRNAs picked-up in the *OsSPL4* gene, gcgctcccctcccctcctct (gRNA1) and agttcccc-cgcgtcgtcgtc (gRNA2), were screened using the CAS-OFFINDER system (http://www.rgenome.net/cas-offinder). The construction was conducted as reported previously (Jiang et al., 2020). The designed targeting sequences were synthesized and annealed to form the oligo adaptors. Vector pBGK032 was digested by *Bsa*I and purified using a DNA purification kit (TransGen Biotech, Beijing, China). A ligation reaction (10 μl) containing 10 ng of the digested plasmid pBGK03 and 0.05 mM oligo adaptor was carried out and directly transformed to *Escherichia coli* competent cells (Kangwei, China) to produce CRISPR/Cas9 constructs (Jiang et al., 2020; Li, Cao, et al., 2019a). The primers are listed in Table S1. The transgenic plants were generated in a Nipponbare background via Agrobacterium (strain GV3101)-mediated transformation (Huang et al., 2014). The transgenic plants were screened using a solution containing 0.1% 6-benzylaminopurine (6-BA) and 50 mg L^{-1} hygromycin. Genomic DNA was extracted from a T_0–T_1 transgenic line and the primers for the SPL4-detect-F/R flanking designed target site (300–500 bp) were used for PCR amplification (Table S1). The products were sequenced directly by Sangon Biotech (Shanghai, China) and BLASTsearched with respect to the WT genome sequence to identify the mutation sites (Figure S7).

M. oryzae inoculation and pathogen infection

The method of *M. oryzae* inoculation was performed as described previously (Li et al., 2017). In brief, the punch-wound leaves detached from three-leaf old seedlings were drop-inoculated with the spores of *M. oryzae* (1×10^5 to 5×10^5 spores per ml) and cultured in H_2O containing 0.1% 6-benzylaminopurine. Alternatively, three-leaf old seedlings were spray-inoculated with the spores (1×10^5 to 5×10^5 spores per ml) and incubated in darkness for 24 h under 100% humidity in the growth room. Then the inoculated samples were continually incubated under a 12:12 h light/dark photocycle with 100% humidity in the growth room. The disease phenotypes were imaged at 5-days post inoculation (d.p.i.). For rice-sheath inoculation assays, 5-cm leaf sheaths were detached from four-leaf stage seedlings and injected with *M. oryzae* strain of GZ8 spore suspension (1×10^5 spores per ml). The injected sheaths were incubated using the same conditions as for spraying inoculation. The infection process of GZ8 in the epidermal layer of the inoculated leaf sheaths was observed by laser scanning confocal microscopy (model A1; Nikon, Tokyo, Japan) at 24 and 36 h.p.i. Simultaneously, the infected rice sheathes were stained by DAB (0.5 mg ml^{-1}) to examine H_2O_2 accumulation.

RT-qPCR assay

Total RNA was extracted from rice samples using TRIzol reagent (Invitrogen, Carlsbad, CA, USA). Then, 1 μg of total RNA was reverse transcribed into cDNA using Primescript RT reagent Kit in accordance with the manufacturer's instructions [TaKaRa Biotechnology (Dalian) Co. Ltd, Shiga, Japan]. In addition, the cDNA required for detection of Osa-miR535 was synthesized with a specific stem-loop primer named miR535-stemloop. Stem-loop RT-qPCR was used to detect and quantify the mature Osa-miR535 with primers miR535-RT-F and Universal-RT-R. snRNA *U6* (U6-F/R) and *OsUbiquitin*. (Ubi-F/R) were used as the internal reference for miRNAs and gene quantification, respectively. RT-qPCR was performed using a SYBR Green PCR Kit (Bimake, Houston, TX, USA). The primers for RT-qPCR in the present study are listed in Table S1.

Transient expression assay in *N. benthamiana*

YFP detection and accumulation was assayed as reported previously. To generate Osa-miR535 target-site reporter fusions, we fused the YFP with the target site of *OsSPL4* at the N-terminus (*35S::SPL4$_{TS}$-YFP*), with *35S::YFP* as a control. The fragments of *SPL4$_{TS}$* were synthesized by annealing gene specific primers

$SPL4_{TS}$-F/R (Table S1) and inserted into the *Kpn*I site of binary vector *pCAMBIA1300-35S*. The constructs were transiently expressed in *N. benthamiana* mediated by Agrobacterium strain *GV3101*. In brief, Agrobacterium strain *GV3101* harboring the respective expression constructs (*35S::SPL4$_{TS}$-YFP, 35S::miR535, 35S::YFP*) was incubated at 28°C for 16 h in LB media containing kanamycin (50 mg ml^{-1}) on a table with shaking at 250 r.p.m. The Agrobacterium were collected at 1000 ***g*** for 4 min and resuspended in MMA buffer [10 mM 2-(*N*-morpholine)-ethanesulphonic acid, 10 mM $MgCl_2$, and 10 mM acetosyringone]. The mixture was allowed to stand at room temperature for 2 h, then infiltrated into *N. benthamiana* leaves. The transient expression assay was performed as described previously (Li et al., 2017). Images were taken using a fluorescence microscope (Axio Imager A2; Carl Zeiss, Jena, Germany) at 48 h.p.i. In western botting analysis, total proteins were extracted using the extraction buffer (50 mM Tris–HCl, pH 7.5, 150 mM NaCl, 1% Triton X-100, 0.1% SDS, 1 mM EDTA, and 1 mM DTT) with 1% protease inhibitor cocktail (04693116001; Roche, Basel, Switzerland). The fusion proteins were detected by anti-GFP (#D110008-0025; Sangon Biotech) with the ECL Western Blot Kit (Clarity™ Western ECL Substrate, #1705061; Bio-Rad, Hercules, CA, USA). The total proteins were stained using Ponceau S as the loading control.

5′ RLM-RACE

5′ RLM-RACE was conducted with the First Choice™ RLM-RACE Kit (Ambion, Austin, TX, USA) in accordance with the manuufacturer's instructions. Total RNA was extracted from 2-week-old seedlings using TRIzol reagent (Invitrogen) in accordance with the manuufacturer's instructions. Nested gene-specific downstream primer sequences are shown in Table S1. The Inner Primer PCR fragments were gel purified and ligated into pEASY-Blunt Simple cloning Vector (CB111; TransGen Biotech) for sequencing to examine the cleavage site.

Y1H assay

The fragment of the *GH3.2* promoter from 724 to 1620-bp containing the GTAC motifs was cloned into the *pHIS2* vector to generate the construct *pHIS2-GH3.2* with primers GH3.2-Y1H-F1/R1. The region of the *GH3.2* promoter from 1 to 744-bp without GTAC motifs was also cloned into the *pHIS2* vector to generate the negative control *pHIS2-GH3.2 m* with primers GH3.2-Y1H-F2/R2. The full-length cDNA sequences of *OsSPL4* (SPL4-FL-F/R) and the *OsSPL4* mutant without SBP domain ($SPL4_{\triangle SBP}$) ($SPL4_{\triangle SBP}$-F/R) was amplified by PCR and cloned into the *pGADT7* vector (Clontech, Mountain View, CA, USA), respectively. Sequences of the primers are listed in Table S1. The fusion constructs were co-transformed into the yeast strain *Y187* yeast cells (Clontech) with the reporter vector (*pHIS2-GH3.2, pHIS2-GH3.2 m*), and grown on SD/–Trp-Leu media for 3 days at 30°C. Then, the interaction was selected on SD/–Trp-Leu-His medium containing 3-aminotriazole. The yeast one-hybrid assays were conducted with Yeast-maker™ Yeast Transformation System 2 (Clontech) in accordance with the manufacturer's instructions. Images were captured using a digital camera (Canon, Tokyo, Japan).

Dual-luciferase assay

The 1619-bp promoter of *GH3.2* was amplified from Nipponbare with primers GH3.2pro-F/R (Table S1) and cloned into the *pCAMBIA1300-LUC* vector to drive the *firefly luciferase gene* (*LUC*) as a reporter construct. *Renilla luciferase* (*REN*) was driven by the CaMV *35S* promoter in the same construct as an internal control. The construct *pCAMBIA1300-SPL4* was used as an effector. Then, these constructs were introduced into the agrobacterium strain GV3101. Agrobacteria harboring the reporter and effector constructs were collected by centrifugation, re-suspended in MS medium [10 mM 2-(*N*-morpholine)-ethanesulphonic acid, 10 mM $MgCl_2$ and 200 μM acetosyringone] until OD_{600} = 0.8 and then incubated at room temperature for 2 h. The mixture of Agrobacterium suspension was infiltrated in *N. benthamiana* leaves. After 3 days under 14:10 h light/dark photocyle conditions, the leaves were infiltrated with 150 μg ml^{-1} luciferin solution (Luciferin Detection Reagent; V8920; Promega, Madison, WI, USA) and kept in the dark for 10 min to quench the fluorescence. Images were captured using a charge-coupled device camera (ChemiDoc XRS+; Bio-Rad). Quantification analysis was performed using a Dual-Lumi™ II Luciferace Reporter Gene Assay Kit (Beyotime) in accordance with the manufacturer's instructions.

EMSA

The SBP-domain of *OsSPL4* ($SPL4_{SBP}$) encoded by the sequences from 193 to 426 bp was amplified using PCR with the primers $SPL4_{SBP}$-F/R. Then, the amplified fragment was purified and inserted into the *pGEX-6p-1* vector to express a glutathione *S*-transferase fusion protein (*GST-SPL4$_{SBP}$*) in Transetta cells (DE3; Transgene Biotech, Beijing, China). The proteins were purified via glutathione sepharose 4B beads (GE Healthcare, Chicago, IL, USA). Oligonucleotide probes containing GTAC motifs were synthesized and labelled (GH3.2pro-EMSA-BiotinF/R) with biotin at the 5′ end, or without biotin (GH3.2pro-EMSA-F/R), by Sangon Biotech. The probe primers are listed in Table S1. The binding reaction contained purified GST-$SPL4_{SBP}$, EMSA/Gel-Shift binding buffer and probes. GST protein alone was used as a negative control. EMSA assay was conducted with the Chemiluminescent EMSA Kit (Beyotime) in accordance with the manufacturer's instructions. The detailed EMSA procedure also followed the manufacturer's instructions. Images were captured using a charge-coupled device camera (ChemiDoc XRS+; Bio-Rad).

ACKNOWLEDGEMENTS

We thank Dr Cai-Lin Lei (Institute of Crop Science, Chinese Academy of Agricultural Sciences) for providing the monogenic resistant lines IRBLkm-Ts. We thank Dr Jing Wang (State Key Laboratory of Crop Gene Exploration and Utilization in Southwest China) for providing the oligonucleotide probes of *WRKY45*. This work was supported by the National Natural Science Foundation of China (no. U19A2033 and 31430072 to Wen-Ming Wang) and the Sichuan Applied Fundamental Research Foundation (2020YJ0332 to Wen-Ming Wang and 2021YJ0304 to Yan Li).

AUTHOR CONTRIBUTIONS

W-MW and YL conceived the project. L-LZ, Y-YH and Y-PZ performed most of the experiments with support from X-XL, S-XZ, X-MY, S-LL, J-LL, S-LZ, HW, Y-PJ, J-WZ, MP, Z-XZ and JF. W-MW, Y-YH and L-LZ contributed to manuscript writing. and editing.

CONFLICT OF INTERESTS

The authors declare no conflict of interest.

DATA AVAILABILITY STATEMENT

All data generated or analyzed during the present study can be found within the manuscript and its supporting materials.

SUPPORTING INFORMATION

Additional Supporting Information may be found in the online version of this article.

Figure S1. Osa-miR535 responds to *Magnaporthe oryzae* and chitin treatment. (a) The expression of Osa-miR535 was examined by stem-loop RT-qPCR upon *M. oryzae* infection in both LTH and IRBLkm-Ts accessions in 4-week-old seedlings. (b) The expression of Osa-miR535 in both LTH and IRBLkm-Ts accessions upon chitin treatment in 4-week-old seedlings. Error bars indicate the SD ($n = 3$). Different letters above the bars indicate significant differences ($P < 0.05$), which are determined by one-way ANOVA analysis followed by post-hoc Tukey's HSD analysis.

Figure S2. Sequence alignment of Osa-miR535 and its target mimic MIM535.

Figure S3. The expression pattern of defense-related genes upon chitin treatment. Defense-related genes, *KS4* (a) and *NAC4* (b), were analyzed by qRT-PCR in 4-week-old seedlings of wild-type (WT) and MIM535 lines at the indicated time points upon chitin and mock treatments. Hpt, hours post treatment. Error bars indicate the SD ($n = 3$). Different letters above the bars indicate significant differences ($P < 0.05$), which are determined by one-way ANOVA analysis followed by post-hoc Tukey's HSD analysis.

Figure S4. Osa-miR535 suppresses the H_2O_2 accumulation upon *Magnaporthe oryzae* inoculation. The leaf sheathes of the indicated lines were subjected to DAB staining at 48 h.p.i. Scale bars = 20 μm. These experiments were repeated twice with similar results.

Figure S5. Sequence alignment of Osa-miR535, Osa-miR156a-j, Osa-miR156i, Osa-miR156k, Osa-miR529a and Osa-miR529b.

Figure S6. The expression levels of *OsSPL4* in T0 OXSPL4 transgenic lines. Four-week-old seedlings of WT and OXSPL4 lines were analyzed by qRT-PCR. WT is Nipponbare used for generating OXSPL4 transgenic plants. 1–18, different individual lines of OXSPL4.

Figure S7. The genotype of *osspl4* mutants. (a) Sequence alignment of the gRNA site of *OsSPL4* gene in *osspl4* mutants and WT. The mutant sites are highlighted in red, '–' indicates the deletion. (b) The sequence peaks of *osspl4* mutants. (c) Protein sequence of *OsSPL4* encoded in *osspl4* mutants.

Figure S8. Schematic and the sequence of the *GH3.2* promoter. Orange marked bars and sequences indicate the positions of GTAC motifs.

Figure S9. The expression of *GH3* family genes in WT, OXSPL4 and *osspl4*. Four-week-old seedlings used for examining gene expression by qRT-PCR. Error bars indicate the SD ($n = 3$). N.D. indicates that the expression of the gene was not detected.

Figure S10. The expression of *WRKY45* is positively regulated by *OsSPL4*. Four-week-old seedlings used for examining gene expression by qRT-PCR. Error bars indicate the SD ($n = 3$). Different letters above the bars indicate significant differences ($P < 0.05$), which are determined by one-way ANOVA analysis followed by post-hoc Tukey's HSD analysis.

Figure S11. The expression of expansin (*EXPA*) genes. Four-week-old seedlings of the indicated rice plants were used to examine gene expression by qRT-PCR. Error bars indicate the SD ($n = 3$). A double asterisk (**) indicates significant differences ($P < 0.01$) via Student's *t* test compared to WT.

Table S1. The primers used in the present study.

REFERENCES

Birkenbihl, R.P., Jach, G., Saedler, H. & Huijser, P. (2005) Functional dissection of the plant-specific SBP-domain: overlap of the DNA-binding and nuclear localization domains. *Journal of Molecular Biology*, **352**, 585–596.

Cardon, G.H., Hohmann, S., Klein, J., Nettesheim, K., Saedler, H. & Huijser, P. (1999) Molecular characterisation of the Arabidopsis SBP-box genes. *Gene*, **237**, 91–104.

Chandran, V., Wang, H., Gao, F., Cao, X.-L., Chen, Y.-P., Li, G.-B. et al. (2019) miR396-OsGRFs module balances growth and rice blast disease-resistance. *Frontiers in Plant Science*, **9**, 1999.

Diederichs, S., Winter, J., Jung, S., Keller, S. & Gregory, R.I. (2009) Many roads to maturity: microRNA biogenesis pathways and their regulation. *Nature Cell Biology*, **11**, 228.

Ding, X., Cao, Y., Huang, L., Zhao, J., Xu, C., Li, X. et al. (2008) Activation of the indole-3-acetic acid–amido synthetase GH3-8 suppresses expansin expression and promotes salicylate-and jasmonate-independent basal immunity in rice. *The Plant Cell*, **20**, 228–240.

Feng, Q., Li, Y., Zhao, Z.X. & Wang, W.M. (2021) Contribution of small RNA pathway to interactions of rice with pathogens and insect pests. *Rice*, **14**, 15.

Franco-Zorrilla, J.M., Valli, A., Todesco, M., Mateos, I., Puga, M.I., Rubio-Somoza, I. et al. (2007) Target mimicry provides a new mechanism for regulation of microRNA activity. *Nature Genetics*, **39**, 1033.

Fu, J., Liu, H., Li, Y., Yu, H., Li, X., Xiao, J. et al. (2011) Manipulating broad-spectrum disease resistance by suppressing pathogen-induced auxin accumulation in rice. *Plant Physiology*, **155**, 589–602.

González-Lamothe, R., El Oirdi, M., Brisson, N. & Bouarab, K. (2012) The conjugated auxin indole-3-acetic acid–aspartic acid promotes plant disease development. *The Plant Cell*, **24**, 762–777.

Hua, Z., Weilong, K., Ziyun, G., Xinyi, F. & Xiaoxiao, D. (2019) Evolutionary analyses reveal diverged patterns of SQUAMOSA promoter binding protein-like (SPL) gene family in *Oryza* genus. *Frontiers in Plant Science*, **10**, 565–565.

Huang, Y.-Y., Shi, Y., Lei, Y., Li, Y., Fan, J., Xu, Y.-J. et al. (2014) Functional identification of multiple nucleocytoplasmic trafficking signals in the broad-spectrum resistance protein RPW8.2. *Planta*, **239**, 455–468.

Jeong, D.H., Park, S., Zhai, J., Gurazada, S.G., De Paoli, E., Meyers, B.C. et al. (2011) Massive analysis of rice small RNAs: mechanistic implications of regulated microRNAs and variants for differential target RNA cleavage. *Plant Cell*, **23**, 4185–4207.

Jiang, M., He, Y., Chen, X., Zhang, X., Guo, Y., Yang, S. et al. (2020) CRISPR-based assessment of genomic structure in the conserved SQUAMOSA promoter-binding-like gene clusters in rice. *The Plant Journal*, **104**, 1301–1314.

Jiao, Y., Wang, Y., Xue, D., Wang, J., Yan, M., Liu, G. et al. (2010) Regulation of OsSPL14 by OsmiR156 defines ideal plant architecture in rice. *Nature Genetics*, **42**, 541.

Lee, R.C., Feinbaum, R.L. & Ambros, V. (1993) The *C. elegans* heterochronic gene lin-4 encodes small RNAs with antisense complementarity to lin-14. *Cell*, **75**, 843–854.

Li, Y., Lu, Y.-G., Shi, Y., Wu, L., Xu, Y.-J., Huang, F. et al. (2014) Multiple rice MicroRNAs are involved in immunity against the blast fungus. *Plant Physiology*, **164**, 1077–1092.

Li, Y., Zhao, S.-L., Li, J.-L., Hu, X.-H., Wang, H., Cao, X.-L. et al. (2017) Osa-miR169 negatively regulates rice immunity against the blast fungus *Magnaporthe oryzae*. *Frontiers in Plant Science*, **8**, 2.

Li, Y., Cao, X.-L., Zhu, Y., Yang, X.-M., Zhang, K.-N., Xiao, Z.-Y. et al. (2019a) Osa-miR398b boosts H_2O_2 production and rice blast disease-resistance via multiple superoxide dismutases. *New Phytologist*, **222**, 1507–1522.

Li, Y., Jeyakumar, J.M.J., Feng, Q., Zhao, Z.-X., Fan, J., Khaskheli, M.I. et al. (2019b) The roles of rice microRNAs in rice-*Magnaporthe oryzae* interaction. *Phytopathology Research*, **1**, 33.

Lin, Z.Z., Jiang, W.W., Wang, J.L. & Lei, C.L. (2001) Research and utilization of universally susceptible property of japonica rice variety Lijiangxintuanheigu. *Scientia Agricultura Sinica*, **34**, 116–117.

Liu, M., Shi, Z., Zhang, X., Wang, M., Zhang, L., Zheng, K. et al. (2019) Inducible overexpression of Ideal Plant Architecture1 improves both yield and disease resistance in rice. *Nature Plants*, **5**, 389–400.

Miura, K., Ikeda, M., Matsubara, A., Song, X.-J., Ito, M., Asano, K. et al. (2010) OsSPL14 promotes panicle branching and higher grain productivity in rice. *Nature Genetics*, **42**, 545.

Naseem, M., Kaltdorf, M. & Dandekar, T. (2015) The nexus between growth and defence signalling: auxin and cytokinin modulate plant immune response pathways. *Journal of Experimental Botany*, **66**, 4885–4896.

Park, C.-H., Chen, S., Shirsekar, G., Zhou, B., Khang, C.H., Songkumarn, P. et al. (2012) The *Magnaporthe oryzae* effector AvrPiz-t targets the RING E3 ubiquitin ligase APIP6 to suppress pathogen-associated molecular pattern–triggered immunity in rice. *The Plant Cell*, **24**, 4748–4762.

Pfeffer, S., Zavolan, M., Grässer, F.A., Chien, M., Russo, J.J., Ju, J. et al. (2004) Identification of virus-encoded microRNAs. *Science*, **304**, 734–736.

Quoc, N.B., Phuong, N.D.N., Trang, H.T.T., Phi, N.B. & Chau, N.N.B. (2019) Expression of osa-miR7695 against the blast fungus *Magnaporthe oryzae* in Vietnamese rice cultivars. *European Journal of Plant Pathology*, **155**, 307–317.

Rogers, K. & Chen, X. (2013) Biogenesis, turnover, and mode of action of plant microRNAs. *The Plant Cell*, **25**, 2383–2399.

Salvador-Guirao, R., Hsing, Y.-I. & San Segundo, B. (2018) The polycistronic miR166k-166h positively regulates rice immunity via post-transcriptional control of EIN2. *Frontiers in Plant Science*, **9**, 337.

Sánchez-Sanuy, F., Peris-Peris, C., Tomiyama, S., Okada, K., Hsing, Y.I., Segundo, B.S. et al. (2019) Osa-miR7695 enhances transcriptional priming in defense responses against the rice blast fungus. *BMC Plant Biology*, **19**, 563.

Sanei, M. & Chen, X. (2015) Mechanisms of microRNA turnover. *Current Opinion in Plant Biology*, **27**, 199–206.

Shao, Y., Zhou, H.Z., Wu, Y., Zhang, H., Lin, J., Jiang, X. et al. (2019) OsSPL3, an SBP-domain protein, regulates crown root development in rice. *Plant Cell*, **31**, 1257–1275.

Shimono, M., Sugano, S., Nakayama, A., Jiang, C., Ono, K., Toki, S. et al. (2007) Rice WRKY45 plays a crucial role in benzothiadiazole-inducible blast resistance. *The Plant Cell*, **19**, 2064–2076.

Sun, M., Shen, Y., Li, H., Yang, J., Cai, X., Zheng, G. et al. (2019) The multiple roles of OsmiR535 in modulating plant height, panicle branching and grain shape. *Plant Science*, **283**, 60–69.

Tang, J. & Chu, C. (2017) MicroRNAs in crop improvement: fine-tuners for complex traits. *Nature plants*, **3**, 17077.

Tsunematsu, H., Yanoria, M.J., Ebron, L., Hayashi, N., Ando, I., Kato, H. et al. (2000) Development of monogenic lines of rice for blast resistance. *Breeding Science*, **50**, 229–234.

Wang, L., Sun, S., Jin, J., Fu, D., Yang, X., Weng, X. et al. (2015) Coordinated regulation of vegetative and reproductive branching in rice. *Proceedings of the National Academy of Sciences*, **112**, 15504–15509.

Wang, H., Jiao, X., Kong, X., Hamera, S., Wu, Y., Chen, X. et al. (2016) A signaling cascade from miR444 to RDR1 in rice antiviral RNA silencing pathway. *Plant Physiology*, **170**, 2365–2377.

Wang, J., Zhou, L., Shi, H., Chern, M., Yu, H., Yi, H. et al. (2018) A single transcription factor promotes both yield and immunity in rice. *Science*, **361**, 1026–1028.

Wang, H., Li, Y., Chern, M., Zhu, Y., Zhang, L.-L., Lu, J.-H. et al. (2021) Suppression of rice miR168 improves yield, flowering time and immunity. *Nature Plants*, **7**, 129–136.

Wightman, B., Ha, I. & Ruvkun, G. (1993) Posttranscriptional regulation of the heterochronic gene lin-14 by lin-4 mediates temporal pattern formation in *C. elegans*. *Cell*, **75**, 855–862.

Xie, K., Wu, C. & Xiong, L. (2006) Genomic organization, differential expression, and interaction of SQUAMOSA promoter-binding-like transcription factors and microRNA156 in rice. *Plant Physiology*, **142**, 280–293.

Yamasaki, H., Hayashi, M., Fukazawa, M., Kobayashi, Y. & Shikanai, T. (2009) SQUAMOSA promoter binding protein–like7 is a central regulator for copper homeostasis in Arabidopsis. *The Plant Cell*, **21**, 347–361.

Yan, Y., Wei, M., Li, Y., Tao, H., Wu, H., Chen, Z. et al. (2021) MiR529a controls plant height, tiller number, panicle architecture and grain size by regulating SPL target genes in rice (Oryza sativa L.). *Plant Science*, **302**, 110728.

Yu, Y., Jia, T. & Chen, X. (2017) The 'how'and 'where'of plant microRNAs. *New Phytologist*, **216**, 1002–1017.

Yue, E., Li, C., Li, Y., Liu, Z. & Xu, J.-H. (2017) MiR529a modulates panicle architecture through regulating SQUAMOSA PROMOTER BINDING-LIKE genes in rice (*Oryza sativa*). *Plant Molecular Biology*, **94**, 469–480.

Zhang, D., Liu, M., Tang, M., Dong, B., Wu, D., Zhang, Z. et al. (2015) Repression of microRNA biogenesis by silencing of OsDCL1 activates the basal resistance to *Magnaporthe oryzae* in rice. *Plant Science*, **237**, 24–32.

Zhang, X., Bao, Y., Shan, D., Wang, Z., Song, X., Wang, Z. et al. (2018) *Magnaporthe oryzae* induces the expression of a MicroRNA to suppress the immune response in rice. *Plant Physiology*, **177**, 352–368.

Zhang, L., Li, Y., Zheng, Y.-P., Wang, H., Yang, X.-M., Chen, J.-F. et al. (2020) Expressing a target mimic of miR156fhl-3p enhances rice blast disease resistance without yield penalty by improving SPL14 expression. *Frontiers in Genetics*, **11**, 327.

Zhao, Z.X., Feng, Q., Cao, X.L., Zhu, Y., Wang, H., Chandran, V. et al. (2019) Osa-miR167d facilitates infection of *Magnaporthe oryzae* in rice. *Journal of Integrative Plant Biology*, **62**, 702–715.

Zhou, M. & Tang, W. (2018) MicroRNA156 amplifies transcription factor-associated cold stress tolerance in plant cells. *Molecular Genetics and Genomics*, **294**, 379–393.

Zhou, S.-X., Zhu, Y., Wang, L.-F., Zheng, Y.-P., Chen, J.-F., Li, T.-T. et al. (2019) Osa-miR1873 fine-tunes rice immunity against *Magnaporthe oryzae* and yield traits. *Journal of Integrative Plant Biology*, **62**, 1213–1226.